JMEPEG (2012) 21:101–104
DOI: 10.1007/s11665-010-9828-5

1059-9495/$19.00

The Effect of Sintering Temperature on Mechanical and Electrical Properties of a W-10Ti Alloy Prepared by Hot Press Sintering

Xianzhuo Jie, Shuhua Liang, Qingxiang Wang, Xin Zhao, Zhikang Fan, and Xianhui Wang

(Submitted March 26, 2010; in revised form November 16, 2010)

W-10Ti alloy was prepared by hot press sintering using W-TiH_2 powders milled for 24 h under argon atmosphere. The effect of sintering temperature on the phase constituents and the microstructure of the alloys was characterized by x-ray diffraction (XRD), scanning electron microscopy (SEM), and transmission electron microscopy (TEM). The microhardness of W-rich phase, electrical resistivity and impurity (C, O) contents of W-10Ti alloy were determined. The results show that the amount of W-Ti solid solution, the microhardness of the W-rich solid solution and the resistance of W-10Ti alloy increase with an increase of sintering temperature. At 1300 °C, W-10Ti alloy has the maximum microhardness value of 333 $HV_{0.05}$, the O content of 360 ppm and C content of 200 ppm.

Keywords electrical resistivity, hot press sintering, impurity contents, microhardness, W-10Ti alloys

1. Introduction

Tungsten-titanium alloys and W-Ti thin films have been extensively studied in the past two decades. It is reported that W-Ti-N (Ref 1), W-Ti-C (Ref 2), and W-Ti-O (Ref 3) thin films can be prepared by the additions of N, C, and O elements into W-Ti alloys. Due to their good corrosion resistance and mechanical properties, W-Ti-N thin films are suitable for stamping or high speed cutting tool materials (Ref 4, 5). W-Ti-O thin films, due to stable electrical and gas sensing properties (Ref 3), can be used as gas sensors. In addition, W-Ti thin films (Ref 6) are widely used in the microelectronic industry as diffusion barrier layers between Al (Ref 7), Cu (Ref 8), and Ag (Ref 9, 10) contact layers and a silicon substrate. Considering the wide use of W-Ti thin films, it is necessary to study the W-Ti alloys in depth. However, at present, most of published studies in the literature (Ref 11, 12) are focused on the properties of W-Ti thin films and there is scant information on the processing and properties of W-Ti alloy by hot press sintering of ball-milled powders. In the present investigation, microhardness of W-rich phase, electrical resistivity and impurity (C, O) contents of W-10Ti alloys were measured, and it was found that W-rich precipitates can form in the Ti-rich regions. The purpose of this investigation is to clarify the effect of sintering temperature on mechanical and electrical properties of a W-10Ti alloy prepared using ball-milled powders and hot press sintering in order to obtain good quality target material which can be suitable for the preparation of W-Ti thin films.

Xianzhuo Jie, Shuhua Liang, Qingxiang Wang, Xin Zhao, Zhikang Fan, and **Xianhui Wang**, School of Materials Science and Engineering, Xi'an University of Technology, No. 5 South Jinhua Road, Xi'an 710048 Shaanxi, China. Contact e-mail: j-x-z00544@163.com.

2. Experimental

The purity, average particle size, and oxygen content of the raw materials are shown in Table 1. W and TiH_2 powders with the mass ratio of 9:1 were put into in a plastic container to mill for 24 h at a ball-to-powder mass ratio of 20:1 under the protection of Ar, and alcohol was added into the jar to balance the cold welding and fracture among the powders as well. The ball-milled W-TiH_2 powders were compacted into cylindrical samples with a diameter of 21 and length of 6 mm in a TM-106 hydraulic machine, followed by sintering at 1100-1300 °C for 1 h in a self-modified hot press furnace under argon atmosphere with the heating rate of 20-25 °C/min.

The phase compositions of the alloys were studied by XRD-7000 and the microstructure of the alloys was characterized by a JSM-6700F field emission scanning electron microscope and a JEM-3010 transmission electron microscope. The microhardness of W-rich phase was tested on TUKON-2100 Vickers. The resistances were measured with a DM-V_2 digital voltmeter and a WYS-3 dc digital display current-stabilized regulator. The sample sizes were 4×4 mm, the mean values were the average of several measured values and the resistance measurements were performed at room temperature. The compositions were determined by an EMGA-620W oxygen-nitrogen analyzer and a CS-344 carbon-sulfur analyzer.

3. Results and Discussion

3.1 XRD Analysis

Figure 1 shows the XRD patterns of W-TiH_2 ball-milled powders and W-10Ti alloy prepared at 1100 °C. It can be seen

that W-TiH_2 ball-milled powders consists of Ti_xW_{1-x} phase (it contains Ti-rich phase and W-rich phase) and a small amount of TiH_2. It suggests that TiH_2 cannot be decomposed during milling. However, no TiH_2 (111) diffraction peak was present in W-10Ti alloy. This can be explained as follows. At elevated temperatures and in the absence of oxygen and nitrogen, TiH_2 can decompose via a series of complex reactions, and result in the release of H_2, and the formation of W-Ti solid solution. Subsequently, no TiH_2 (111) and Ti (110) diffraction peaks occur in the W-Ti alloy prepared at 1100 °C.

Table 1 Parameters of raw materials

Material	Purity, %	Average particle size, μm	Oxygen content, ppm
W powder	≥ 99.9	6	≤ 600
TiH_2 powder	≥ 99.7	35	≤ 2000

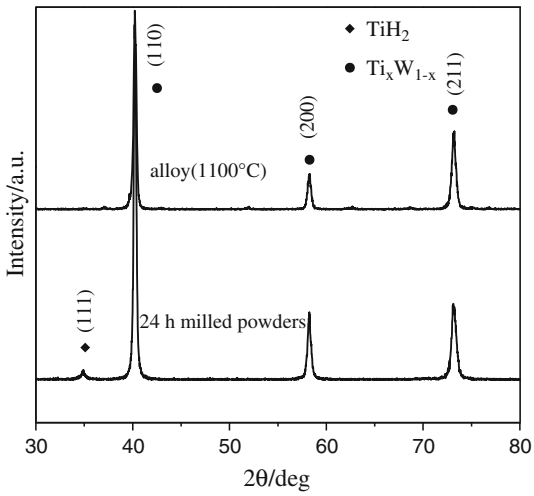

Fig. 1 XRD patterns of W-TiH_2 ball-milled powders and W-10Ti alloy prepared at 1100 °C

3.2 Microstructure

The scanning electron microscopic (SEM) images of W-TiH_2 powders ball-milled for 24 h and W-10Ti alloys prepared at 1100 and 1200 °C are shown in Fig. 2(a), 2(b), and 2(c), respectively. As seen from Fig. 2(a), W-TiH_2 ball-milled powders exist in the form of lamellar and blocky shapes. At the initial stage of ball milling, W and TiH_2 particles are broken and their powder sizes decrease. With the progress of milling, higher energy is generated among powders, and the alcohol added can reduce the surface energy of powders, which inhibit the cold welding effectively. Meanwhile, the liquid alcohol can separate W-TiH_2 powders, and prevent the edges of the powders from fracturing.

W-10Ti alloy consisted of a large amount of W-rich and a small amount of Ti-rich solid solution. The microstructure of W-10Ti alloy has a main lamellar structure, the gray regions represent W-rich solid solution while the black regions represent Ti-rich solid solution. A large amount of W-Ti solid solution can be seen, as ball milling process can refine crystal grain and reduce diffusion distance, the diffusion between W and Ti becomes easier and more sufficient. From Fig. 2(b), it can be seen that some of the lamina are deformed obviously under the action of pressure and temperature, the width of lamina is about 1-5 μm with the aspect ratio between 4:1 and 2:1 and a large amount of W-rich precipitates are formed in

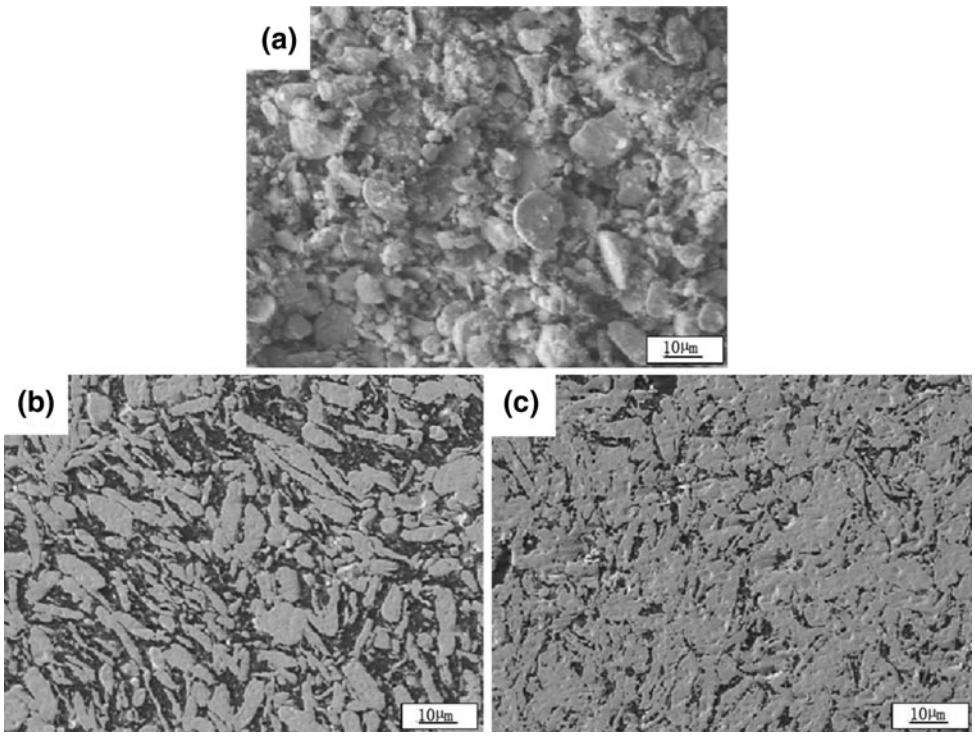

Fig. 2 Secondary electron images of W-Ti powders milled for 24 h and W-10Ti alloys prepared at 1100 and 1200 °C (a) the ball-milled powders, (b) the material sintered at 1100 °C, and (c) the material sintered at 1200 °C

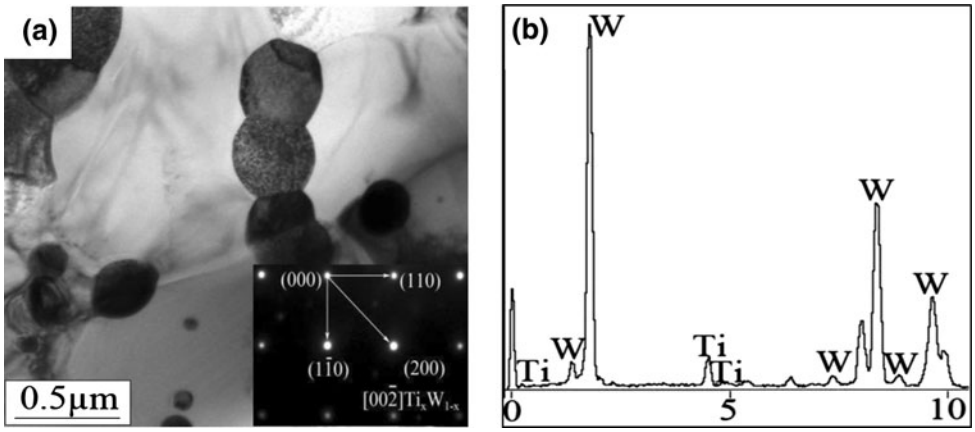

Fig. 3 (a) TEM micrograph and electron diffraction pattern of W-rich phase and (b) EDS spectra of black particle

Ti-rich regions. It is also found that W-Ti solid solution content increases with increase of sintering temperature. After milling for 24 h, both surface energy and micro-defects of W-Ti powders increase, and thus, promotes the reaction between W and Ti and the formation of a large amount of W-rich solid solution with an increase of sintering temperature.

Figure 3 shows transmission electron microscopic (TEM) image of W-10Ti alloy prepared at 1100 °C. As seen from Fig. 3(a), bright area represents Ti-rich solid solution, and dark grains are the W-rich phase. This can be determined by the electron diffraction pattern (Fig. 3a) and EDS result (Fig. 3b). The EDS result shows that the dark grains are consisted of a large amount of W element and a small amount of Ti element, indicating they may be W-rich phase, and this can be further determined by the indexing of electron diffraction pattern. This finding is in good accordance with the work of Lo et al. (Ref 13). According to W-Ti binary phase diagram, Ti and W can form an infinite solid solution at above 1250 °C. With the increase of sintering temperature, the diffusion occurs between W and Ti, which results in the formation of W-Ti solid solution. However, β-Ti will transform to hcp-Ti structure during cooling and the solid solution content of hcp-Ti and W is lower than that of β-Ti and W, so W-rich precipitates are formed in the Ti-rich phase.

3.3 Microhardness

W-rich phase is desired because the W-rich solid solution is the mainly substance as W-Ti target material for sputtering. The effect of sintering temperature on the microhardness of W-rich solid solution is illustrated in Fig. 4. It can be seen that the microhardness increases with an increase of sintering temperature. At high temperature, W-10Ti alloy begins to soften, gas releases continuously and different particle sites are rearranged. Meanwhile, the voids and defects of W-10Ti alloy decrease under the pressure. With the decrease of voids and the growth of new inter-granular, the microhardness increases. During the sintering process, substitution reaction happens between W and Ti. Moreover, W and Ti atoms can fill these vacancies continuously and higher temperature promotes the formation of W-rich solid solution, which has a higher microhardness than W matrix, and thus, improve the microhardness of W-rich phase to some extent. As discussed above, with the increase of sintering temperature, the formation of large amounts of W-rich solid solution leads to larger microhardness.

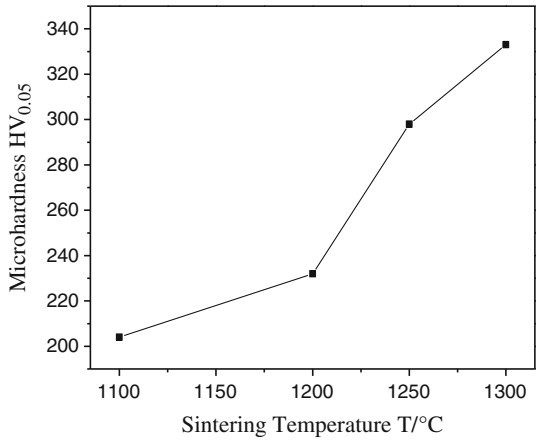

Fig. 4 Variation of microhardness with sintering temperature for W-rich solid solution

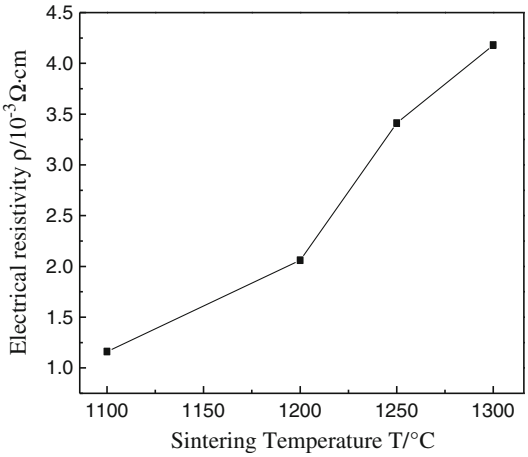

Fig. 5 Variation of electrical resistivity with W-Ti alloys prepared at different sintering temperature

3.4 Electrical Resistivity

Figure 5 shows the electrical resistivity of W-10Ti alloy prepared at different sintering temperatures. It can be seen that the electrical resistivity of W-10Ti alloy increases with the

increase of sintering temperature. Since the second-phase solute (Ti) dissolve into solvent (W), the original crystal lattice is destroyed and more distortions are generated, which destroys the periodicity of lattice potential field and improves the probability of electron scattering, and finally increases the electrical resistivity of W-10Ti alloy. In addition, with the increase of sintering temperature, the thermal vibration of crystal lattice ion and the electronic scattering effect of the foreign atom, the dislocation and point defects are improved, which can reduce the electrical conductibility of W-10Ti alloy.

3.5 Impurity Contents

It has been reported that the purity of target materials have a great effect on the performance of sputtered thin films (Ref 11). The higher the purity of the alloy, the better the performance of the sputtered thin films will be. Hence, the impurity contents of target materials and pollution source of thin films should be reduced to improve the performance of thin films. In order to clarify the purity contents of W-Ti alloys prepared at different temperatures, the contents of C and O for W-10Ti alloy prepared at 1100 and 1300 °C were measured, respectively. At 1100 °C, C and O contents are 280 and 430 ppm, respectively, while, at 1300 °C, C and O contents are 200 and 360 ppm, respectively. It is evident that impurity contents of W-10Ti alloy will reduce with an increase of temperature. It can be explained as follows. More H_2 can be decomposed from TiH_2 at higher temperature, which can react with C and O, and the reaction products ($CxHy$, H_2O) can be removed with the floating Ar gas. The results show that C and O contents decreased with the increasing sintering temperature.

4. Conclusions

The effect of sintering temperature has a significant effect on the microstructure, electrical resistivity, microhardness, and impurity contents of W-10Ti alloy prepared by hot press sintering. With the increasing sintering temperature, the electrical resistivity of W-10Ti alloy and the microhardness of W-rich solid solution are improved, while the impurity contents decrease. W-10Ti alloy is mainly consisted of W-Ti solid solution phase, and the fraction of W-Ti solid increases with an increase of sintering temperature. It is also found that W-rich precipitates can form in the Ti-rich regions.

References

1. L.R. Shaginyan, M. Misina, J. Zemek, J. Musil, F. Regent, and V.F. Britun, Composition, Structure, Micro-Hardness and Residual Stress of W-Ti-N Films Deposited by Reactive Magnetron Sputtering, *Thin Solid Films*, 2002, **408**(1–2), p 136–147
2. W.S. Jung, H.Y. Lee, K.H. Nam, and J.G. Han, The Synthesis of W-Ti-C Films With a Control of Element Composition by Hybrid System, *Surf. Coat. Technol.*, 2005, **200**(1–4), p 721–725
3. E. Comini, G. Sberveglieri, and V. Guidi, Ti-W-O Sputtered Thin Film as n-or p-Type Gas Sensors, *Sens. Actuators B Chem.*, 2000, **70**(1–3), p 108–114
4. P.N. Silva, J.P. Dias, and A. Cavaleiro, Tribological Behaviour of W-Ti-N Sputtered Thin Films, *Surf. Coat. Technol.*, 2005, **200**(1–4), p 186–191
5. A. Cavaleiro, B. Trindade, and M.T. Vieira, Influence of Ti Addition on the Properties of W-Ti-C/N Sputtered Films, *Surf. Coat. Technol.*, 2003, **174–175**, p 68–75
6. S. Petrović, N. Bundaleski, D. Peruško, M. Radović, J. Kovač, M. Mitrić, B. Gaković, and Z. Rakočević, Surface Analysis of the Nanostructured W-Ti Thin Film Deposited on Silicon, *Surf. Sci.*, 2007, **253**(12), p 5196–5202
7. T. Hara, N. Ohtsuka, K. Sakiyama, and S. Saito, Barrier Effect of W-Ti Interlayers in A1 Ohmic Contact Systems, *Trans. Electron Devices*, 1987, **34**(3), p 593–598
8. A.G. Dirks, R.A.M. Wolters, and A.J.M. Nellissen, On the Microstructure-Property Relationship of W_Ti_(N) Diffusion Barriers, *Thin Solid Films*, 1990, **193–194**(Part 1), p 201–210
9. S.K. Bhagat, H. Han, and T.L. Alford, Tungsten-Titanium Diffusion Barriers for Silver Metallization, *Thin Solid Films*, 2006, **515**(4), p 1998–2002
10. S.K. Bhagat, N.D. Theodore, and T.L. Alford, Thermal Stability of Tungsten-Titanium Diffusion Barriers for Silver Metallization, *Thin Solid Films*, 2008, **516**(21), p 7451–7457
11. V.G. Glebovsky, V. Yu Yaschak, V.V. Baranov, and E.L. Sackovich, Properties of Titanium-Tungsten Thin Films Obtained by Magnetron Sputtering of Composite Cast Targets, *Thin Solid Films*, 1995, **257**(1), p 1–6
12. P.N. Silva, J.P. Dias, and A. Cavaleiro, Performance of W-Ti-(N) Coated Pins in Lubricated Pin-On-Disk Tests, *Surf. Coat. Technol.*, 2008, **202**(11), p 2338–2343
13. C.F. Lo and P. Gilman, Particle Generation in W-Ti Deposition, *J. Vac. Sci. Technol. A*, 1999, **17**(2), p 608–610